REVISTA
ÁGUAS SUBTERRÂNEAS

Assessment of groundwater hydrochemical properties and irrigation water quality using GIS in the Tolga Region, South-East Algeria

Avaliação das propriedades hidroquímicas das águas subterrâneas e da qualidade da água para irrigação utilizando SIG na região de Tolga, sudeste da Argélia

Mohamed Khelalfa[1], Nora Bouchahm[2], Saliha Ben Aoun[3]

[1]Department of Civil Engineering and Hydraulic. Faculty of Architecture, Urbanism, Civil Engineering and Hydraulics. Mohamed Khider University, Biskra- Algeria, m.khelalfa@centre-univ-mila.dz
[2]Scientific and Technical Research Center on Arid Regions, Biskra – Algeria, bouchahm_nora@yahoo.fr
[3]Scientific and Technical Research Center on Arid Regions, Biskra – Algeria, salihabenaoun@yahoo.fr

Received:
March 14, 2026
Received in revised form:
March 22, 2026
Accepted:
March 22, 2026
Available online:
July 21, 2026
Section:
Articles

Keywords:
Groundwater.
Irrigation.
Water quality.
IWQI.
Gibbs diagram.
GIS.

Palavras-chave:
Água subterrânea.
Irrigação.
Qualidade da água.
IQAI.
Diagrama de Gibbs.
SIG.

https://doi.org/10.14295/ras.v40i2.30402

ABSTRACT

Groundwater is the primary water source in arid and semi-arid regions due to the scarcity of surface resources and irregular rainfall. making the assessment of its quality essential to ensure sustainable use in agriculture. Despite the importance of groundwater for irrigation, previous studies have not applied an integrated approach combining hydrochemical sample classification according to Gibbs diagrams, calculation of the Irrigation Water Quality Index (IWQI) for each category and spatial analysis using Geographic Information Systems (GIS). This study aimed to assess groundwater quality for irrigation and analyze the spatial variability of the IWQI in the Tolga region, southeastern Algeria, using hydrochemical analysis and geostatistical modeling. Samples were classified into two main types: rock-affected and evaporation-affected with dominant hydrochemical processes identified using Gibbs diagrams. IWQI classification results indicated that rock-affected samples fall within low and moderate restriction classes, whereas evaporation-affected samples are categorized into high and severe restriction classes, highlighting the crucial role of evaporation in determining irrigation water suitability and its direct impact on operational constraints. Spatial distribution maps revealed a clear northwest–southeast gradient in IWQI values for rock-affected samples associated with geological formations, while evaporation-affected samples showed a simpler pattern with only two main zones. The results confirm that the spatial variability of groundwater quality is primarily influenced by geological factors and evaporation processes, emphasizing the importance of integrating hydrochemical analysis with GIS to understand water distribution and support sustainable management of agricultural resources.

RESUMO

A água subterrânea é a principal fonte de água em regiões áridas e semiáridas devido à escassez de recursos superficiais e à irregularidade das chuvas, o que torna essencial avaliar sua qualidade para garantir o uso sustentável na agricultura. Apesar da importância da água subterrânea para irrigação estudos anteriores não aplicaram uma abordagem integrada que combine a classificação das amostras hidroquímicas de acordo com os diagramas de Gibbs, o cálculo do Índice de Qualidade da Água de Irrigação (IQAI) para cada categoria e a análise espacial usando Sistemas de Informação Geográfica (SIG). Este estudo teve como objetivo avaliar a qualidade da água subterrânea para irrigação e analisar a variabilidade espacial do IQAI na região de Tolga, no sudeste da Argélia, utilizando análise hidroquímica e modelagem geoestatística. As amostras foram classificadas em dois tipos principais: afetadas por rochas e afetadas pela evaporação, com processos hidroquímicos dominantes identificados por meio dos diagramas de Gibbs. Os resultados da classificação do IQAI indicaram que as amostras afetadas por rochas se enquadram nas classes de restrição baixa e moderada, enquanto as amostras afetadas pela evaporação são categorizadas nas classes de restrição alta e severa, destacando o papel crucial da evaporação na determinação da adequação da água para irrigação e seu impacto direto nas limitações operacionais. Mapas de distribuição espacial revelaram um claro gradiente noroeste–sudoeste nos valores do IQAI para as amostras afetadas por rochas associado às formações geológicas, enquanto amostras afetadas pela evaporação exibiram um padrão mais simples com apenas duas zonas principais. Os resultados confirmam que a variabilidade espacial da qualidade da água subterrânea é influenciada principalmente por fatores geológicos e processos de evaporação, enfatizando a importância de integrar a análise hidroquímica com SIG para entender a distribuição da água e apoiar a gestão sustentável dos recursos agrícolas.

INTRODUCTION

Groundwater is the primary water source in arid and semi-arid regions due to the scarcity of surface resources and irregular rainfall making the assessment of its quality essential to ensure sustainable use, particularly in agriculture (Tang *et al.*, 2023; Hamma *et al.*, 2024). Its hydrochemical properties are influenced by both natural and anthropogenic factors, such as geological formations, evaporation, ion exchange processes, and intensive agricultural activities (Tang *et al.*, 2023; El-Haddad *et al.*, 2024).

The assessment of groundwater suitability for irrigation relies on several hydrochemical indicators, including sodium percentage (Na%), sodium adsorption ratio (SAR), and total salinity, in addition to the Irrigation Water Quality Index (IWQI), provides a comprehensive evaluation of water quality. Furthermore, integrating hydrochemical analysis with Geographic Information Systems (GIS) and modern statistical approaches has improved understanding of the spatial variability of groundwater quality and supported sustainable management of water resources in arid and semi-arid regions (Fadl *et al.*, 2024; Tian *et al.*, 2025).

Groundwater in the Tolga region, southeastern Algeria, is a vital resource supporting agricultural activities and meeting the water needs of the local population in a semi-arid environment lacking stable surface water resources (Rechachi *et al.*, 2025). Studies have reported elevated salinity levels and the presence of certain metallic elements in these waters, influenced by climatic conditions and land use patterns, along with salinization and soil and water degradation in some oases highlighting the importance of monitoring and sustainable management of these resources (Khelalfa; Bouchahm; Chaib, 2024; Zouaoui *et al.*, 2022; Belghemmaz *et al.*, 2021).

Although several recent studies have assessed groundwater quality for irrigation using the (IWQI) and GIS in semi-arid regions of Algeria and worldwide, none have applied a fully integrated approach combining hydrochemical sample classification according to Gibbs or Piper plots. IWQI calculation for each hydrochemical category, and spatial mapping. Locally, Laoufi *et al.* (2025) evaluated groundwater quality in a semi-arid agricultural area using IWQI and GIS to assess nitrate contamination. but the samples were not classified according to Gibbs plots. Similarly, Mansouri *et al.* (2025) applied a method combining IWQI, GIS, and machine learning without Gibbs plot classification for each sample category. Other studies in Algeria, such as Messaid *et al.* (2025) and Ababakr *et al.* (2023), focused on hydrochemical analysis, GIS, or IWQI separately, without integrating all three components. Globally, studies such as Nefla *et al.* (2026), Eid *et al.* (2023), and Alrowais *et al.* (2026) applied IWQI and GIS to evaluate water quality, but they did not calculate IWQI for each sample category according to Gibbs plots nor link the results to spatial mapping. Similarly, Mishra *et al.* (2025) focused on spatio-temporal hydrogeochemical characterization using GIS and multivariate statistics, with partial use of Gibbs plots. but did not implement the fully integrated method

Therefore, the precise research gap in the Tolga region, southeastern Algeria, lies in the absence of any study that applies a fully integrated approach combining hydrochemical sample classification according to Gibbs plots, IWQI calculation for each class, and spatial mapping using GIS**.** Applying this method represents a novel and original contribution for the region and provides accurate tools to support sustainable management of water and agricultural resources. This study aims to analyze the impact of evaporation and water–rock interactions on the IWQI of groundwater in the Tolga region using the Gibbs plot to identify hydrochemical processes and examining the spatial distribution of water quality through GIS**.**

Study area and data

The Tolga region located in the northern Algerian Sahara within Biskra Province (between latitudes 34°30′ and 35°00′ N and longitudes 5°00′ and 5°30′ E). is the study area of this research (Figure 1). It is characterized by a hot desert climate. with plains and plateaus favorable for infiltration and the recharge of alluvial aquifers.

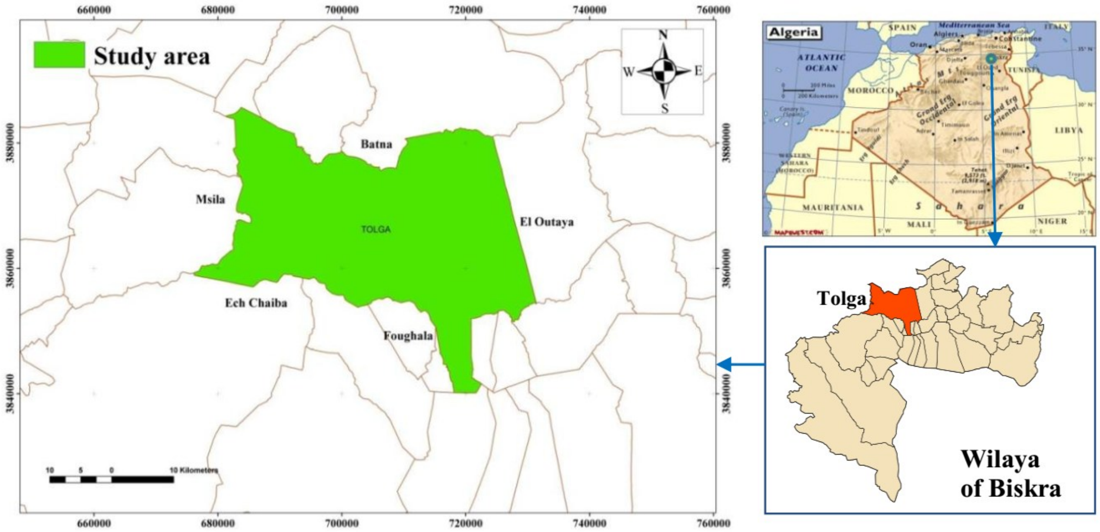

Figure 1. Map of the administrative situation of the Tolga region (SE Algerian).

Geology and Hydrogeology

From a geological perspective, the stratigraphic sequence of the study area is organized, from bottom to top, into Albian, Upper Senonian, Lower Eocene, Mio-Pliocene, and Quaternary formations (Farès *et al.,* 2023). This lithostratigraphic succession strongly controls the architecture of the aquifer systems and the modalities of groundwater flow in the Tolga–Biskra region (Castany, 1982; OSS, 2003).

The region hosts three major aquifer systems: the Intercalary Complex (CI)**,** the Terminal Complex (CT)**,** and the Quaternary deposits (QD)**.** The Intercalary Complex, mainly developed within the Albian formations, consists of sands, sandstones, and rock debris intercalated with clay and gravel layers. Its relatively high porosity and transmissivity make it a deep, regionally extensive aquifer, playing a strategic role in water supply for Saharan areas (Guendouz *et al.,* 2003; UNESCO, 1972).

The Terminal Complex represents a multilayered aquifer system, extending within the carbonate formations of the Upper Senonian and Lower Eocene, as well as the sandy Mio-Pliocene levels (Fatoum, 2017). The fissured Lower Eocene limestones, locally associated with marls and dolomitic limestones of the Upper Senonian, promote preferential groundwater flow through fracture networks and structural discontinuities.

The Quaternary phreatic aquifer is a shallow groundwater reservoir developed within Quaternary alluvial deposits, mainly composed of sands, gravels, and silts (Chebbah. 2007). This formation represents a shallow aquifer that is generally exploited for local irrigation and the water supply of rural areas and oases in the Ziban plain. Its depth is relatively low and varies across different locations, with a thickness generally limited compared to deeper aquifers (Miopliocene, Eocene, or Intercalary Complex), and it is characterized by low spatial continuity**.**

The hydraulic interactions between these different reservoirs, controlled by lithology, fracturing, and arid to semi-arid climatic conditions, significantly influence the chemical quality and spatio-temporal evolution of groundwater in the study area (Guendouz *et al.,* 2003; Castany, 1982).

Materials and methods

To carry out this study ,the following steps were followed.

Source, nature, and parameters of the data

The present study is based on the exploitation of hydrochemical data derived from a previous investigation, comprising 35 groundwater wells distributed across the Tolga region (Biskra. Algeria) (Khelalfa; Bouchahm; Chaib, 2024). The physicochemical parameters considered include the major cations (Ca^{2+}, Mg^{2+}, Na^{+}, and K^{+}), the major anions (Cl^-, HCO_3^-, and NO_3^-), as well as general parameters such as pH. electrical conductivity (EC), total dissolved solids (TDS), and total hardness (TH) (Table 4).

A representative sampling strategy was designed according to the depth of each borehole. The spatial distribution of the boreholes was as follows: 11 in the southern sector, 5 in the northern sector near the Saharan Atlas foothills, 1 in the western sector (the only borehole available), 13 in the eastern sector, and 5 in the central sector (Figure 2).

Laboratory analyses were conducted in two locations: the eleven southern boreholes were examined at the Algérienne des Eaux (AOWB) laboratory in Biskra, whereas the remaining twenty-four boreholes were analyzed at the Centre de Recherche Scientifique et Technique sur les Régions Arides (CRSTRA), also located in Biskra. All boreholes are labeled from P1 to P35.

Based on these parameters, several indices of irrigation water quality were calculated, particularly the Sodium Adsorption Ratio (SAR). The sampling conditions, analytical methods, and characteristics of the wells, including borehole depth, were described in detail in the reference study and are therefore not redeveloped in the present work.

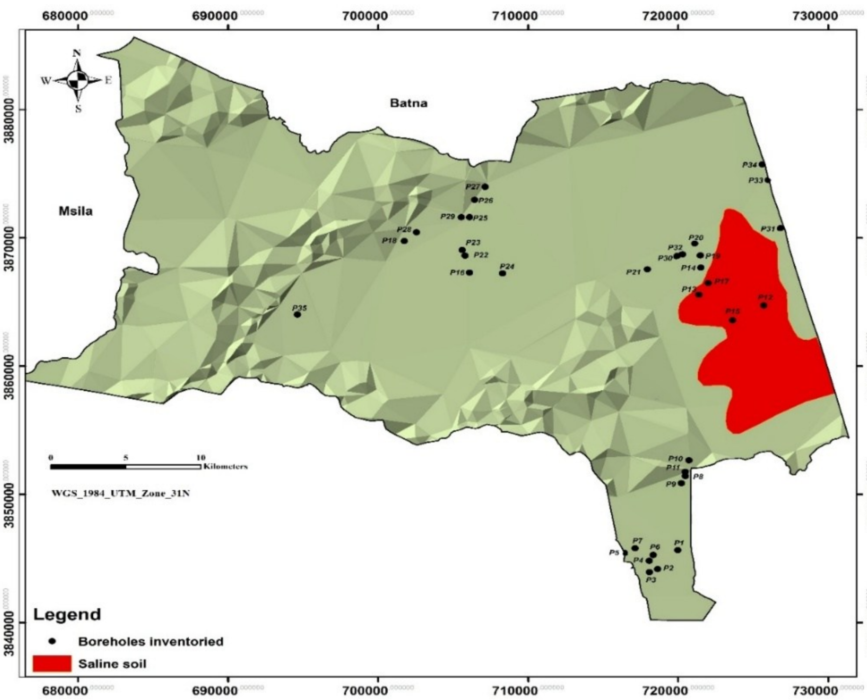

Figure 2. Map showing the inventory of aquifer boreholes

Classification of samples

To further investigate the hydrochemical mechanisms, the samples were classified using the Gibbs diagram (Gibbs, 1970). This classification made it possible to identify two main groups: the first group consisting of 11 samples mainly influenced by the evaporation effect, and the second group comprising 24 samples dominated by lithology (rock dominance). This distribution is illustrated in Table 7 and spatially located in Figure 3**.**

The distinction between these two types of samples forms the basis for calculating IWQI thereby providing a better understanding of the factors controlling groundwater quality in the studied region.

Calculation of water quality indices

The IWQI was calculated using key irrigation-related parameters (SAR, EC, Na^+, Cl^-, and HCO_3^-) for each sample, following the method proposed by Meireles *et al.* (2010). The results obtained allowed the classification of water according to the irrigation water quality classes defined by Meireles *et al.* (2010)**.** The value of IWQI was calculated:

$$IWQI = \sum \left[\left(\frac{W_i}{\sum_{i=1}^{n} W_i} \right) \left(q_{i\max} - \left(\frac{(\chi_{ij} - \chi_{\inf}) \times (q_{iamp})}{\chi_{amp}} \right) \right) \right] \quad (1)$$

where: qimax = the maximum value of each class as shown in Table 3;
χij = the measured value of the parameter;
χinf = the minimum value of the next class for the parameter;
qiamp = the range (amplitude) of the classes;
χamp = the corresponding value to which the parameter belongs.

The Sodium Adsorption Ratio (SAR) was calculated using the following formula (Richard, 1954):

$$SAR = \frac{Na}{\sqrt{\frac{Ca + Mg}{2}}} \quad (2)$$

Table 1 shows the parameters and their corresponding weights (Wi) used in the calculation of the IWQI (Meireles *et al*., 2010). Table 2 presents the classification of groundwater quality according to the IWQI proposed by Meireles *et al*. (2010), indicating the corresponding water quality ranges and types for irrigation purposes. Table 3 presents the water quality values (qi) for each groundwater sample, calculated based on the parameter criteria established by Ayers and Westcot (1999), allowing a comprehensive evaluation of irrigation water suitability.

Table 1 – Parameters and weights (Wi) used for IWQI calculation

Parameters	(Wi)
EC (µS/cm)	0.211
Na^+ (meq/l)	0.204
HCO_3^- (meq/l)	0.202
Cl^- (meq/l)	0.194
SAR	0.189

Table 2 – Classification of water quality ranges and types according to the IWQI (Meireles *et al*., 2010)

IWQI	Restrictions for water use
0–40	Severe restriction [SR]
40–55	High restriction [HR]
55–70	Moderate restriction [MR]
70–85	Low restriction [LR]
85–100	No restriction [NR]

Table 3 – Values of rated water quality (qi) according to different parameter criteria (Ayers; Westcot, 1999)

qi	EC (µs/cm)	Na+ (meq/l)	HCO3- (meq/l)	Cl- (meq/l)	SAR (-)
From 85 to 100	From 200 to 750	From 2 to 3	From 1 to 1.5	< From 4	< From 3
From 60 to 85	From 750 to 1500	From 3 to 6	From 1.5 to 4.5	From 4 to 7	From 3 to 6
From 35 to 60	From 1500 to 3000	From 6 to 9	From 4.5 to 8.5	From 7 to 10	From 6 to 12
From 0 to 35	From 200< > From 3000	From 2< > From 9	From 1< > From 8.5	> From 10	> From 12

GIS Mapping of Water Quality Indices

The IWQI was mapped using a GIS to visualize the spatial distribution of irrigation water quality. For each sample, an individual map was created based on the coordinates of the inventoried wells, and spatial interpolation methods (kriging) were applied to generate continuous maps, allowing the identification of areas with optimal or problematic water quality.

The kriging spatial interpolation method was applied using ArcGIS**.** Kriging is a geostatistical technique based on the theory of regionalized variables, which considers both the distance and the degree of spatial dependence between measured points to estimate values at unsampled locations. The experimental semivariogram was calculated for each hydrochemical parameter, and several theoretical models were fitted, including Spherical, Gaussian, Exponential, and Circular models.

Anisotropy was applied to account for directional variations, and model parameters, including nugget, sill, and range, were optimized to ensure the best spatial prediction performance. To evaluate the accuracy of the results, cross-validation was performed by comparing predicted values with measured values at sampling points, and the model with the lowest prediction error was selected to ensure reliable estimates.

The kriging method was chosen because it relies on spatial correlation between sampling points and provides accurate and unbiased estimates, unlike deterministic methods such as Inverse Distance Weighting (IDW), which do not account for the spatial structure of the data. This choice is supported by Isaaks and Srivastava (1989) and Webster and Oliver (2007)**.**

Results and discussion

Table 4 presents the descriptive statistics for all samples before their classification into evaporation and rock-dominated groups, including the Mean, Min, Max, Standard Deviation (SD), and Coefficient of Variation (CV) for all ions and hydrochemical indices. It provides an overview of chemical variability and serves as a basis for sample classification according to the Gibbs diagram (Tables 5 and 6).

Table 4 – Statistical parameters of physicochemical elements and SAR (Overall sample of 35 boreholes)

Parameters	EC (mS/cm)	TDS (mg/l)	TH (mg/l)	pH (-)	Ca^{2}+ (mg/l)	Mg^{2}+ (mg/l)	Na+ (mg/l)	K+ (mg/l)	HCO_3- (mg/l)	Cl- (mg/l)	NO_3- (mg/l)	SAR (-)
Means	2.983	1493.3	982.02	7.96	218.79	106.00	369.62	6.73	210.54	346.25	34.12	5.20
Min	0.930	465.00	486.50	7.36	88.00	51.55	51.11	1.08	56.12	92.30	4.04	0.90
Max	7.64	3820.0	2739.8	8.69	548.00	333.60	1708.7	28.00	287.92	1192.8	124.77	23.60
	1.571	784.88	478.50	0.32	117.10	54.44	357.92	5.46	50.04	243.16	24.25	4.94
CV	0.53	0.53	0.49	0.04	0.54	0.51	0.97	0.81	0.24	0.70	0.71	0.95

Source: (Khelalfa; Bouchahm; Chaib, 2024).

Mechanism for acquiring the chemical characteristics of borehole water

The Gibbs diagram is widely used as an effective tool to identify the geochemical processes responsible for groundwater mineralization (Murhula *et al.*, 2019; Allia *et al.*, 2018). Figure 3 shows that the chemical composition of most well water samples in the Tolga area, with a total of 35 samples, is mainly influenced by the rock weathering process, which accounts for about 24 samples. This process involves interactions between water and rocks that lead to the dissolution of minerals and the release of ions into groundwater, thereby altering its chemical characteristics. The remaining eleven samples are strongly influenced by evaporation, particularly in the central and eastern parts of the region. In these areas, water loss through evaporation leads to an increase in the concentration of dissolved salts in the groundwater. This effect reflects the arid to semi-arid nature of the local climate and high evaporation rates. which influences groundwater quality**.** This distribution reflects the combined influence of geological and climatic factors on groundwater quality across different parts of the study area.

Tables 5 and 6 present the descriptive statistics of the major ions and hydrochemical indices for the two groups. namely the evaporation-dominated group and the rock-dominated group, including the Mean, Min, Max, SD, and CV. These data result from the classification of samples according to the Gibbs diagram and provide a detailed overview of the variation of chemical parameters within each group before analyzing the observed differences.

The two tables provide a detailed comparison between the evaporation-dominated and rock-dominated groups. based on the mean values of each hydrochemical variable. It is evident that the evaporation group exhibits higher values for all major ions (Ca^{2+}, Mg^{2+}, Na^+, K^+, HCO_3^-, Cl^-, NO_3^-) as well as for salinity indices (EC, TDS, TH, SAR) compared to the rock-dominated group, while pH remains practically constant between the two groups.

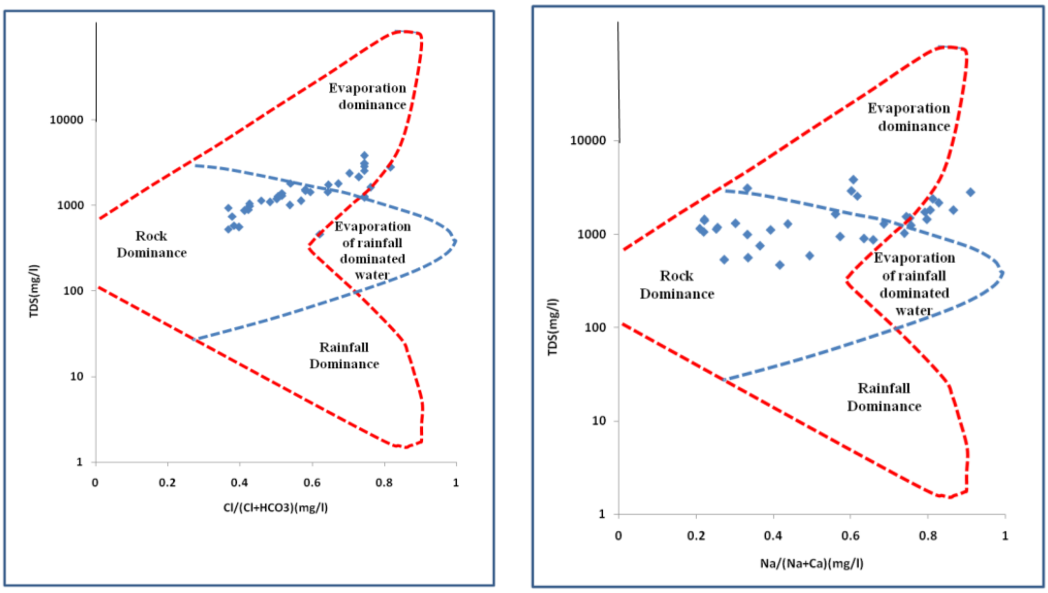

Figure 3. Gibbs diagram. mechanisms for controlling borehole water quality

Table 5 – Statistical parameters of physicochemical parameters and SAR Evaporation-dominated group (11 boreholes)

Parameters	EC (mS/cm)	TDS (mg/l)	TH (mg/l)	pH -	Ca^{2+} (mg/l)	Mg^{2+} (mg/l)	Na^+ (mg/l)	K^+ (mg/l)	HCO_3^- (mg/l)	Cl^- (mg/l)	NO_3^- (mg/l)	SAR (-)
Mean	4.85	2425.00	1349.17	7.99	282.26	156.40	748.29	7.10	231.55	607.84	49.81	9.76
Min	3.26	1630.00	645.62	7.65	120.00	84.00	220.00	3.04	134.20	326.60	11.73	2.29
Max	7.64	3820.00	2742.60	8.26	548.00	333.60	1708.76	28.00	287.92	1192.80	124.77	23.60
SD	1.37	686.56	652.23	0.18	153.22	71.25	381.91	7.04	55.15	239.67	29.00	5.76
Cv	0.28	0.28	0.48	0.02	0.54	0.46	0.51	0.99	0.24	0.39	0.58	0.59

Table 6 – Statistical parameters of physicochemical variables and SAR for the rock-dominated samples (24 boreholes)

Parameters	EC (mS/cm)	TDS (mg/l)	TH (mg/l)	pH (-)	Ca^{2+} (mg/l)	Mg^{2+} (mg/l)	Na^+ (mg/l)	K^+ (mg/l)	HCO_3^- (mg/l)	Cl^- (mg/l)	NO_3^- (mg/l)	SAR (-)
Mean	2.12833	1066.42	815.33	7.94	189.69	82.90	196.06	6.56	200.91	226.35	26.93	3.11
Min	0.93	465.00	487.00	7.36	88.00	51.55	51.11	1.08	56.12	92.30	4.04	0.90
Max	3.05	1525.00	1281.83	8.69	352.71	131.28	532.64	16.00	256.20	511.20	55.40	9.12
SD	0.63172	316.85	246.65	0.37	85.18	20.06	161.10	4.73	45.52	121.25	18.21	2.62
Cv	0.29682	0.30	0.30	0.05	0.45	0.24	0.82	0.72	0.23	0.54	0.68	0.84

This overall difference reflects a clear variation in water chemical composition, with the evaporation group representing more concentrated waters for all components, whereas the rock group corresponds to less concentrated waters. The tables also show that these differences are consistent across all variables and are not limited to any specific ion or indicator, thus providing clear and direct evidence of the chemical characteristics' divergence between the two groups when considering mean values**.**

Table 7 presents the Gibbs diagram classification of the wells indicating whether each well is influenced by rock weathering or evaporation. An additional column provides the depth of each inventoried well as supplementary information.

Figure 4 illustrates the spatial distribution of all sampled wells in the study area. Wells from the evaporation-dominated group are shown in red, while those from the rock-dominated group are shown in blue. This map allows for an immediate visualization of the geographical distribution of the two groups and serves as a basis for interpreting the hydrochemical variations observed in the previous tables. The results of the IWQI calculation and the classification of irrigation use restrictions are summarized in Tables 8 and 9. showing the evaporation-influenced samples and the rock–water interaction-dominated samples. respectively. with a clear ranking according to this index.

Table 7 – Gibbs-based classification and depth of the inventoried boreholes

Name of boreholes	Classification	Depth (m)	Name of boreholes	Classification	Depth (m)
P1	Rock dominance	150	P27	Rock dominance	120
P2		150	P28		100
P3		90	P29		130
P4		150	P30		65
P5		220	P32		150
P6		300	P35		170
P7		300	P8	Evaporation dominance	185
P9		185	P12		220
P10		310	P14		200
P11		300	P15		180
P13		80	P16		100
P18		92	P17		150
P19		180	P20		150
P21		100	P23		120
P22		116	P31		145
P24		100	P33		150
P25		94	P34		150
P26		120			

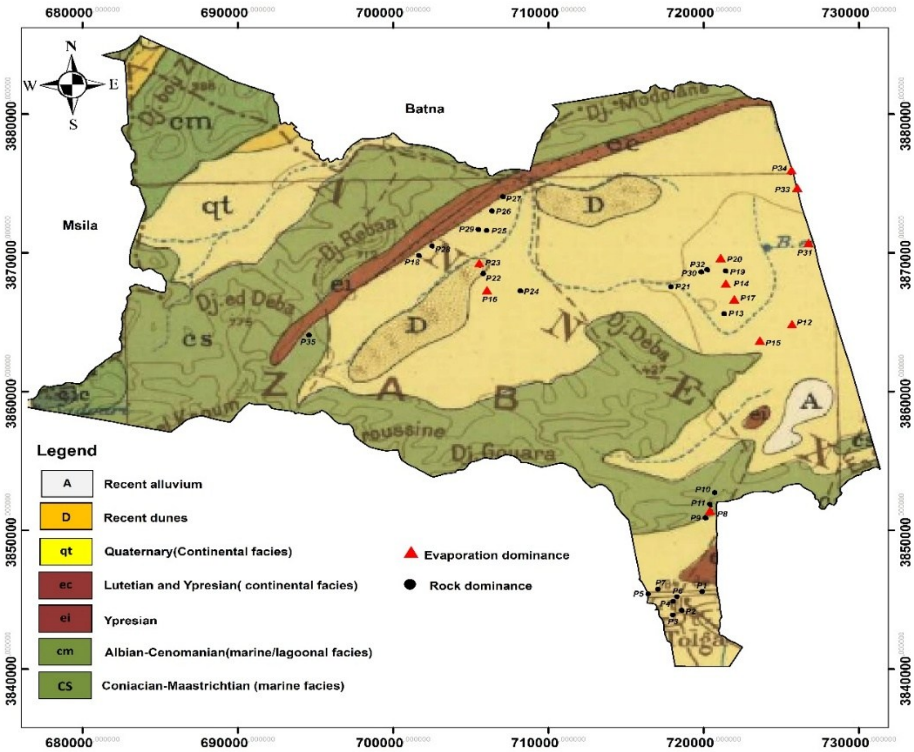

Figure 4. Spatial distribution of groundwater samples according to dominant hydrochemical processes (rock-dominated vs. evaporation-dominated) over the Geological Map of the Study Area (modified after the Geological Map of Algeria, 1952).

The IWQI value of sample P23 (47.8) is higher than that of the other samples in the evaporation-dominated group. According to Yang *et al*. (2022), its position near the rock-dominated domain on the Gibbs diagram reflects a combined influence of evaporation and rock–water interaction. which explains its better ionic balance (Fig. 8).

Samples P13, P19, P21, and P32, although classified within the rock-dominated domain according to the Gibbs diagram (see Figure 8), show IWQI values close to those of evaporation-dominated samples (Figure 5). Conversely, sample P23, despite being classified within the evaporation-dominated domain according to the Gibbs diagram (see Figure 9), exhibits an IWQI value like rock-dominated samples. These results indicate the presence of transitional zones where rock–water interaction or evaporation predominates, but both processes contribute to the water chemistry reflecting a mixed influence on water irrigation quality.

Table 8 – Assessment of Irrigation Water Quality Using IWQI and Restriction Classification for Evaporation-Affected Samples

Sample	IWQI	Restrictions
P8	42.10	[HR]
P12	36.97	[SR]
P14	38.74	[SR]
P15	15.6	[SR]
P16	36.9	[SR]
P17	32.59	[SR]
P20	30.8	[SR]
P23	47.8	[HR]
P31	34.4	[SR]
P33	40.6	[HR]
P34	41.96	[HR]

Table 9 – Assessment of Irrigation Water Quality Using IWQI and Restriction Classification for rock-Affected Samples

Sample	IWQI	Restrictions	Sample	IWQI	Restrictions
P1	61.60	[MR]	P19	37	[SR]
P2	72	[LR]	P21	40	[HR]
P3	71	[LR]	P22	63	[MR]
P4	62.8	[MR]	P24	63	[MR]
P5	67	[MR]	P25	71	[LR]
P6	69	[MR]	P26	59	[MR]
P7	68	[MR]	P27	63	[MR]
P9	73	[LR]	P28	65	[MR]
P10	65	[MR]	P29	70	[MR]
P11	79	[LR]	P30	42	[HR]
P13	31	[SR]	P32	38	[SR]
P18	55	[HR]	P35	58	[MR]

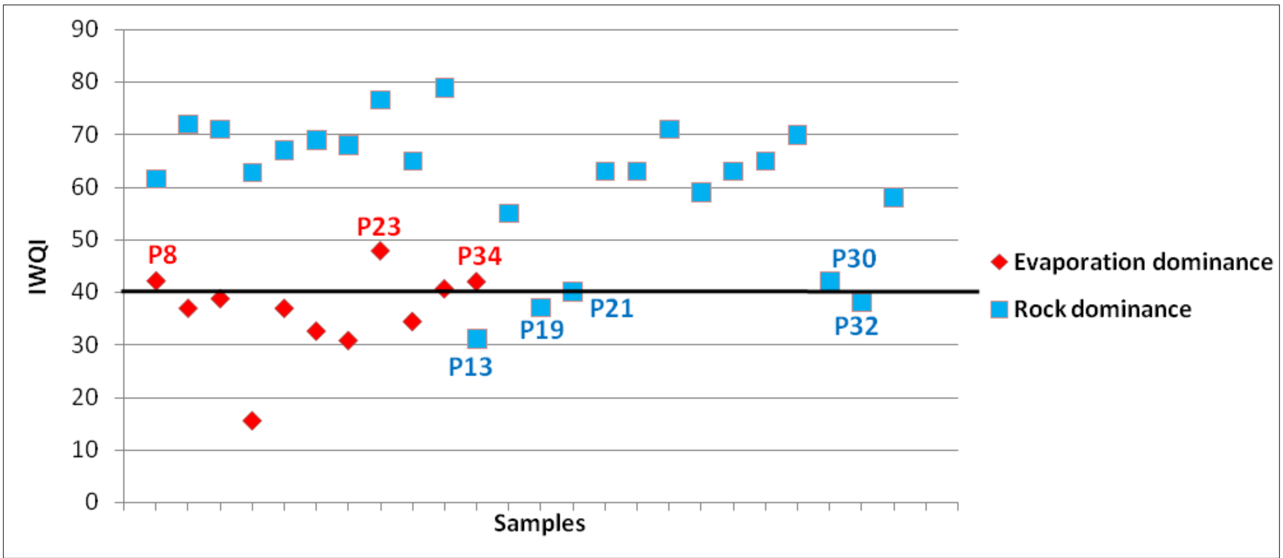

Figure 5. Variation of the Irrigation Water Quality Index (IWQI) in samples affected by evaporation and rock–water interaction.

From the analysis of transitional samples, such as P13, P19, P21, P32, and P23, it was observed that some samples are in mixed zones between rock-dominated and evaporation-dominated influences, with IWQI values that do not fully correspond to their classification in the Gibbs diagram. These observations prompted us to use linear correlation analysis between IWQI and chemical parameters (EC, Na, Cl, SAR), as this approach allows us to assess the contribution of each variable to water quality and identify which factors have the greatest influence on variability within these transitional zones. thereby providing a more accurate understanding of the relationship between chemical composition and mixed hydrogeological areas.

Figures 6 and 7 illustrate the results of this analysis, with Figure 6 representing the samples classified within the rock-dominated domain, while Figure 7 shows the samples classified within the evaporation-dominated domain.

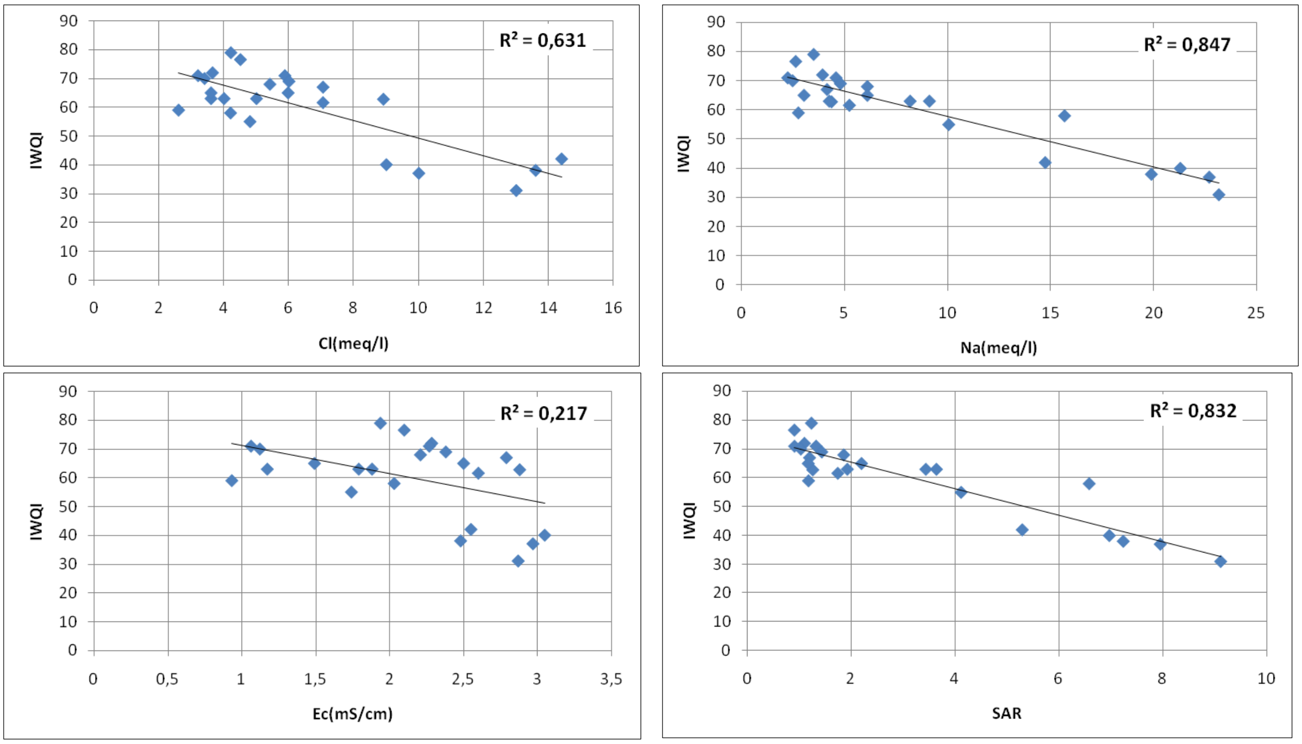

Figure 6. Correlation Analysis of IWQI with EC. SAR. Na. and Cl in Rock Water Samples

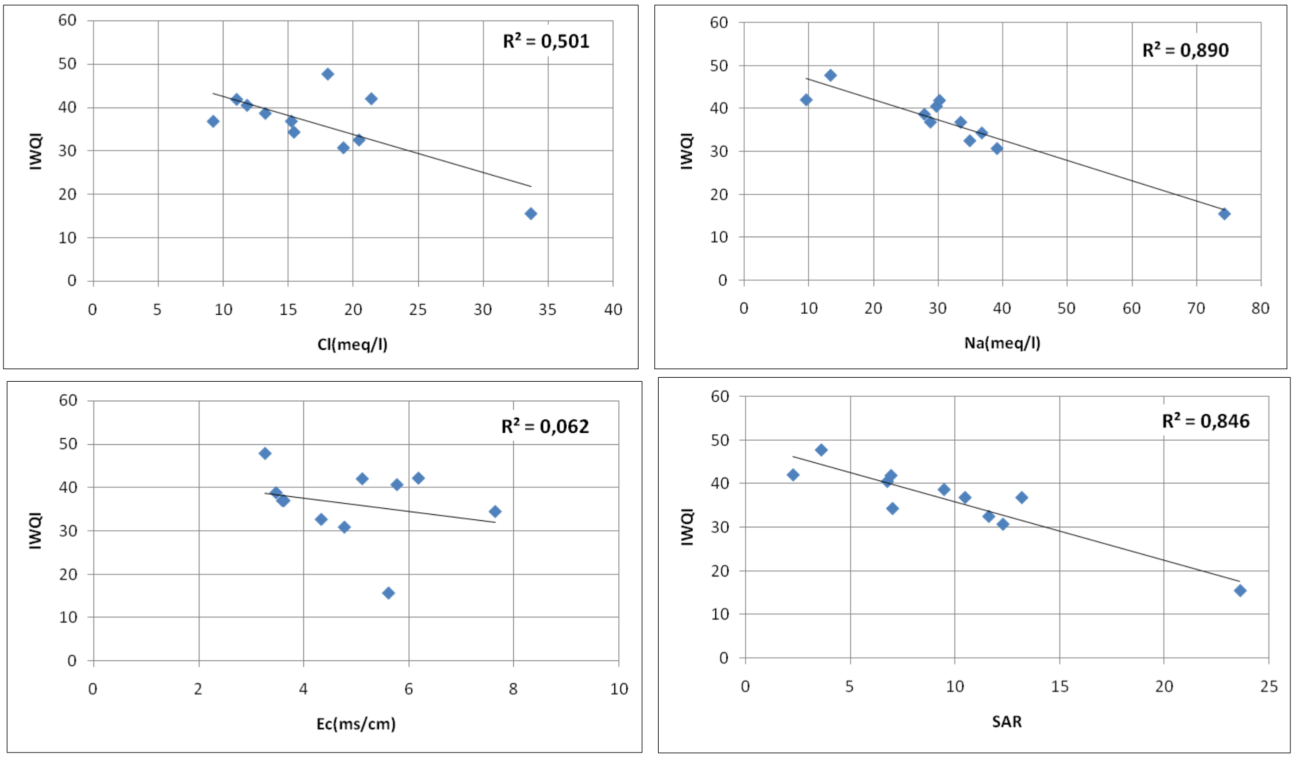

Figure 7. Correlation Analysis of IWQI with EC. SAR. Na. and Cl in Evaporated Water Samples

The linear correlation analysis between the IWQI and the chemical parameters revealed clear differences in the strength of the relationships depending on the variable and the type of samples. For rock-dominated samples, the correlation with sodium (Na) was (R^2=0.847) and with the Sodium Adsorption Ratio (SAR) (R^2=0.832), while the correlation with chloride (Cl) was moderate (R^2=0.631) and with electrical conductivity (EC) very weak (R^2=0.217). For evaporation-dominated samples, the correlation was very strong with Na (R^2=0.890) and SAR (R^2=0.846), moderate to strong with Cl (R^2=0.501), and very weak with EC (R^2=0.062). These results indicate that IWQI is mainly influenced by Na and SAR, whereas the total salinity (EC) plays a minor role in this index.

The Gibbs diagram provides a classification of the samples according to the dominant process controlling water chemistry (rock-water interaction or evaporation), but it does not directly show the effect of Na and SAR on IWQI. Overall, most rock-dominated samples have IWQI values above 40, while most evaporation-dominated samples have values below 40, with a few mixed samples (one rock-dominated and four evaporation-dominated) located in transitional zones between the two influences. These mixed samples explain the deviation of IWQI behavior from the purely rock or evaporation classification. highlighting the importance of combining chemical analysis with the Gibbs diagram to better understand water quality.

Table 10 presents the classification of water samples according to the Irrigation Water Quality Index (IWQI) including the two samples affected by evaporation and rock–water interaction.

Table 10 – Classification of Water Samples According to (IWQI)

Echantillon	IWQI	Restriction	Numbre of Semple	Percentage %
Rock Affected Samples	0-40	SR	2	8.33
	40-55	HR	4	16.66
	55-70	MR	12	50
	70-85	LR	6	25
	85-100	NR	(-)	0
Evaporation Affected Samples	0-40	SR	7	63.63
	40-55	HR	4	36.36
	55-70	MR	(-)	0
	70-85	LR	(-)	0
	85-100	NR	(-)	0

The data in Table 10 show that rock-affected samples are mainly distributed in the moderate restriction (MR) class (50%). followed by the low restriction (LR) class (25%), while the high (16.66%) and severe (8.33%) restriction classes represent smaller proportions.

In contrast, evaporation-affected samples are entirely distributed in the severe restriction (63.63%) and high restriction (36.36%) classes. with no samples recorded in the moderate or low restriction categories.

Variographic treatment and validation of fit results

The experimental semivariogram was fitted using four different models (Tables 11 and 12), with kriging weights derived from the variogram. Model performance was evaluated through cross-validation which showed high reliability: the Mean Error (ME) and Mean Standardized Error (MSE) were close to zero, the Root Mean Squared Error (RMSE) closely aligned with the Average Standard Error (ASE), and the Standardized RMSES values approached one.

Together, these indicators confirm that the selected model is appropriate for spatial interpolation in accordance with ESRI (2005) guidelines. The parameters of the fitted variogram models and the cross-validation statistics used to evaluate the performance of the interpolation model for IWQI are presented in Tables 11 and 12**.**

The variogram parameters indicate a clear difference in the spatial structure of the IWQI values between the two sample groups. For the rock-affected samples, the Nugget/Sill ratio (0.061) shows strong spatial dependence. Suggesting that water quality variations are primarily controlled by local geological factors.

In contrast, the evaporation-affected samples exhibit a higher Nugget/Sill ratio (0.59)**,** indicating moderate spatial dependence and greater spatial variability, likely influenced by environmental processes such as evaporation and climatic factors. The Nugget/Sill ratio is an important geostatistical indicator used to assess the degree of spatial dependence; values below 0.25 typically indicate strong spatial correlation, whereas values between 0.25 and 0.75 reflect moderate dependence (Cambardella *et al*., 1994; Webster; Oliver, 2007; Isaaks; Srivastava, 1989)**.**

The cross-validation results indicate that the kriging model for IWQI is reliable, with all five error indicators ME, MSE, ASE, RMSE, and RMSES showing good performance. According to ESRI (2005) guidelines, these results confirm that the model meets the acceptance criteria for spatial interpolation.

Table 11 – Parameters of the fitted variogram models used for IWQI interpolation

IWQI	Range (Km)	Partial Sill	Nugget	Nugget/Sill	Number of classes	Angle (°)	Type of kriging	Type of variogram
Rock Affected Samples	28.57	271.12	17.75	0.061	12	65.91	Ordinary	Gaussian
Evaporation Affected Samples	71.15	36.93	53.31	0.59	12	74.70	Ordinary	Exponential

Table 12 – Cross-validation statistics for the kriging interpolation of IWQI.

IWQI	Size	ME	MSE	ASE	RMSE	RMSES
Rock-Affected Samples	24	0.121	0.027	5.97	5.87	1.09
Evaporation Affected Samples	11	-0.005	0.018	8.628	8.879	0.974

Spatial variability mapping by kriging interpolation

Figure 8 shows the distribution map of the IWQI for samples influenced by rock weathering. Wells P13, P19, P21, and P32 are in areas corresponding to the end of rock dominance on the Gibbs plot. The spatial distribution map of the IWQI for rock-affected samples reveals a clear gradient, with values gradually decreasing from the northwestern to the southeastern part of the study area, where the lowest water quality is observed. This decline is primarily attributed to the presence of evaporitic formations, particularly halite, which increases the concentration of dissolved salts in groundwater through water–rock interactions, as reported by Brinis and Boudoukha (2011). Conversely, higher IWQI values are observed in the southern part, particularly in the deep wells P9, P10. and P11, which may indicate that these wells are connected to a different aquifer system or receive recharge from a separate hydrogeological source, although this hypothesis requires further hydrological data for confirmation. Geostatistical analysis further supports this spatial pattern, as the variogram shows a Nugget/Sill ratio of 0.061 (<0.25), indicating strong spatial dependence of IWQI values. This demonstrates that the spatial variability of irrigation water quality is largely controlled by the geological distribution of rocks and lithological characteristics across the study area.

Figure 9 shows the distribution map of the IWQI for evaporation-affected samples, with the location of well P23 in the zones of the end of evaporation dominance on the Gibbs plot. The spatial distribution map of the IWQI for samples affected by evaporation reveals a simple spatial pattern, represented by the presence of two main zones within the studied area, where one of the zones exhibits relatively similar IWQI values compared to the other. This pattern reflects the limited spatial variability of IWQI values, indicating a degree of uniformity in the hydrochemical conditions associated with the evaporation process across most parts of the region. Geostatistical analysis supports this observation, as the experimental variogram showed a Nugget/Sill ratio of 0.59, indicating a moderate spatial dependence. This level of spatial dependence is primarily related to the low overall variability in the data due to the convergence of IWQI values among the studied wells, which explains the emergence of a simple spatial pattern consisting of only two main zones on the interpolation map.

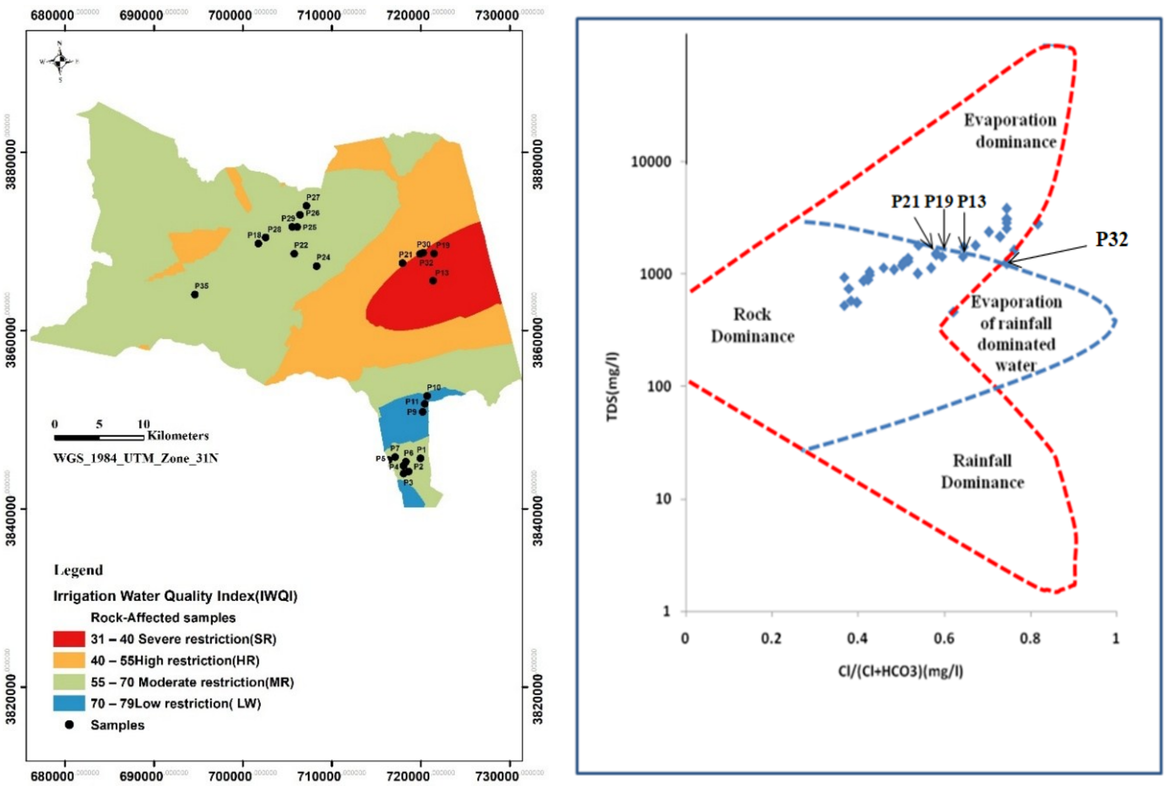

Figure 8. Distribution map of the IWQI for rock-dominated samples.

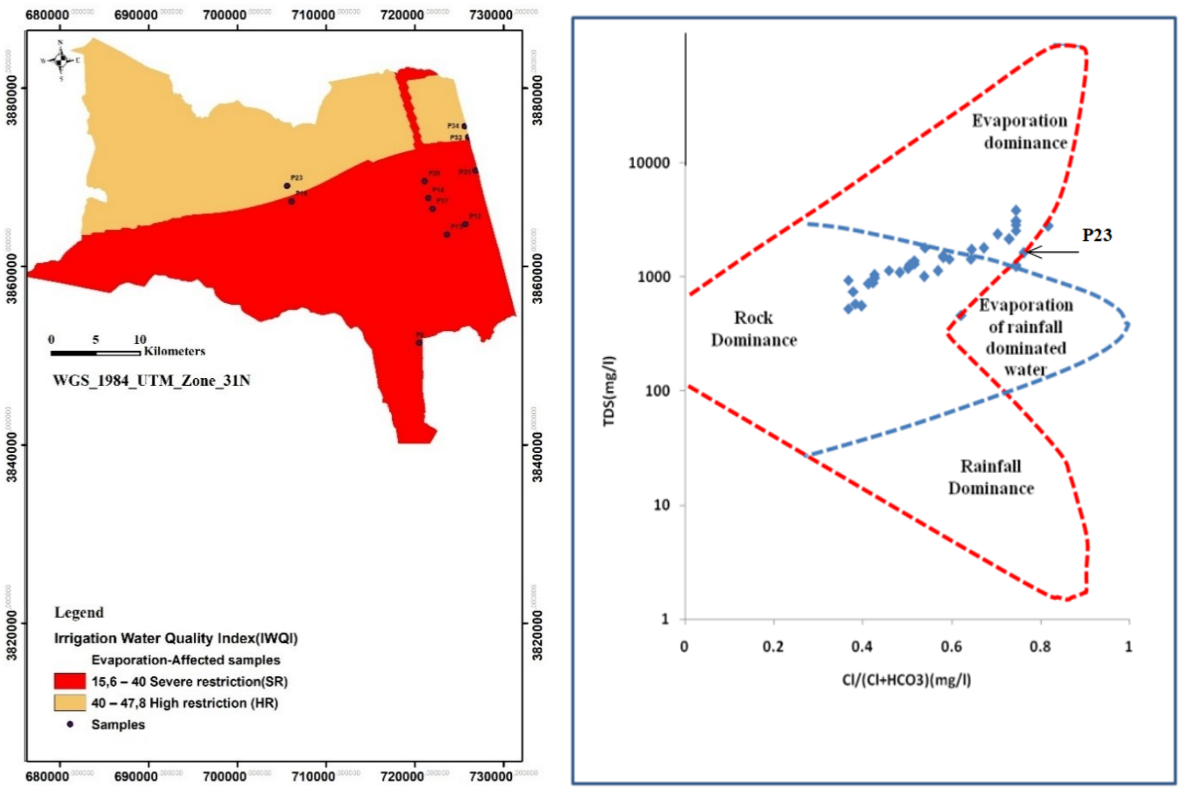

Figure 9. Distribution map of the IWQI for evaporation-dominated samples.

Conclusions

The study revealed clear chemical differences between rock-affected and evaporation-affected groundwater samples. with the latter exhibiting higher concentrations of various chemical components, highlighting the impact of different geochemical processes on groundwater composition in the area.

The Irrigation Water Quality Index (IWQI) showed that rock-affected samples were mainly classified within the moderate and low restriction categories for irrigation, whereas all evaporation-affected samples fell into the high and severe restriction categories, indicating the significant role of evaporation in reducing water suitability for irrigation.

The correlation between the IWQI and chemical parameters varies with sample type. For rock-dominated samples, the correlation with sodium (Na) and sodium adsorption ratio (SAR) was high, while the correlation with chloride (Cl) was moderate and with electrical conductivity (EC) very weak. In evaporation-dominated samples, the correlation with Na and SAR was very strong. moderate to strong with Cl. and very weak with EC.

Spatial distribution maps of IWQI indicated a clear northwest-to-southeast gradient for rock-affected samples, while evaporation-affected samples exhibited a simpler pattern with only two main zones. reflecting limited spatial variability in IWQI values.

Geostatistical analysis supported these observations, showing strong spatial dependence for rock-affected samples (Nugget/Sill = 0.061) and moderate dependence for evaporation-affected samples (Nugget/Sill = 0.59), suggesting that spatial variability of groundwater quality is largely controlled by geological formations and local processes such as evaporation.

Overall, the study emphasizes the critical influence of geological formations and evaporation processes on irrigation groundwater quality and highlights the importance of integrating hydrochemical analysis, IWQI, and geostatistical methods with GIS-based spatial mapping to support sustainable groundwater resource management in arid and semi-arid regions.

REFERÊNCIAS

ABABAKR, F. A.; AHMED, K. O.; AMINI. A.; KARAMI MOGHADAM. M.; GÖKÇEKUŞ, H. Spatio-temporal variations of groundwater quality index using geostatistical methods and GIS. **Applied Water Science**, [*s. l.*], v. 13, 206, 2023. DOI: https://doi.org/10.1007/s13201-023-02010-4.

ALLIA, Z.; CHEBBAH, M.; OUAMANE, A. Analysis and evaluation of groundwater quality of the Miocene-Pliocene aquifer system in the zab chergui. lown septentrional sahara. **Courrier du Savoir**, [*s. l.*], n. 26, p. 235-244, 2018.

ALROWAIS, R.; ABDEL-DAIEM, M. M.; MAKLAD, M. A.; OUNAIES, W.; SAID, N. Hydrogeochemical and GIS-Integrated Evaluation of Drainage Water for Sustainable Irrigation Management in Al-Jouf. Saudi Arabia. **Water**, [*s. l.*], v. 18, n. 1, p. 78, 2026. DOI: https://doi.org/10.3390/w18010078

AYERS. R.S.; WESTCOT. D. W. **Water quality for agriculture**. Rome: Food and Agriculture Organization of the United Nations, 1999. (FAO Irrigation and Drainage Paper, 29, Rev. 1)

BELGHEMMAZ, S.; FENNI, M.; AFRASINEI, G. M.; LOUADJ, Y. Soil and water salinization of an oasis ecosystem in the Ziban region (Tolga). Algeria. **Trends in Earth Observation**, [*s. l.*], n. 2. p. 45–50, 2021.

BRINIS, N.; BOUDOUKHA, A. Classification statistique et hydrochimique des eaux souterraines de la plaine d'el-outaya. (w) de Biskra-Algérie. **Courrier du Savoir,** [*s. l.*], n.11, p. 41-46, mar. 2011.

CAMBARDELLA, C. A.; MOORMAN, T. B.; PARKIN, T. B.; KARLEN, D. L.; NOVAK, J. M.; TURCO, R. F. Field-scale variability of soil properties in central Iowa soils**. Soil Science Society of America Journal**, [*s. l.*], v. 58, n. 5, p.1501–1511,1994. DOI: http://doi.org/10.2136/sssaj1994.03615995005800050033x.

CASTANY, G. **Principes et méthodes de l'hydrogéologie**. Paris: Dunod, 1982.

CHEBBAH, M. **Lithostratigraphie. sédimentologie et modèles de bassins des dépôts néogènes de la région de Biskra. de part et d'autre de l'accident sud atlasique (Zibans. Algérie).** 2007. Thèse (Doctorat d'État) - Université Mentouri Constantine, Algérie, 2007.

EID, M. ; ELBAGORY, M.; TAMMA, A. A.; GAD, M.; ELSAYED, S.; HUSSEIN, H.; MOGHANM, F. S.; OMARA, A. E. D; KOVÁCS, A.; SZŰCS. P. Evaluation of groundwater quality for irrigation in deep aquifers using multiple graphical and indexing approaches supported with machine learning models and GIS techniques. Souf Valley. Algeria. **Water**, [*s. l.*], v. 15, n. 1, p. 182, 2023. DOI: https://doi.org/10.3390/w15010182

ESRI. **ESRI Annual Report and Review of Research for the Year Ended 31 December 2003**. Dublin. Ireland: Environmental Systems Research Institute, 2005. Available in: https://www.esri.ie/publications/esri-annual-report-and-review-of-research-for-the-year-ended-31-december-2003

FADL, M. E.; ELFADL, D. M. A.; HUSSIEN, E. A. A. ; ZEKARI, M. ; SHAMS, E. M.; DROSOS, M.; SCOPA, A.; MEGAHED, H. A. 'Irrigation water quality assessment in Egyptian arid lands utilizing irrigation water quality index and geo-spatial techniques'. **Sustainability**, [*s. l.*], v. 16, n. 14, p. 6259, 2024. DOI: https://doi.org/10.3390/su16146259.

KESSASRAA, F.; MEZERREGE, N. El H.; DEHIBIB, D. E.; DJARETB, L.; BOUHCHICHAD, A.; MESBAH, M. Hydrogeological characterization of the Complex Terminal aquifer using geoelectrical investigation in the arid environment of Chetma-Biskra (South-East of Algeria). **Acque Sotterranee**: Italian Journal of Groundwater, Pavia, v. 12, n. 1, p. 39-51, 2023. DOI: https://doi.org/10.7343/as-2023-608

FATOUM, B. **Diagnostic de la qualité des eaux souterraines et superficielles de la région de Biskra.** Thèse (Doctorat en sciences hydrauliques) - Université de Biskra, Biskra, 2017.

GIBBS, R. J. Mechanisms Controlling World's Water Chemistry. **Science**, [*s. l.*], n. 170, p.1088–1090, 1970.

GUENDOUZ, A.; MOULLA, A. S.; EDMUNDS, W. M.; SHAND, P.; ZOUARI. K. Groundwater evolution in the Continental Intercalaire aquifer of southern Algeria and Tunisia**. Applied Geochemistry**, [*s. l.*], v. 18, n. 6, p.805–822, 2003.

HAMMA, B.; ALODAH, A.; BOUAICHA, F.; BEKKOUCHE, M. F.; BARKAT, A.; HUSSEIN. E. E. 'Hydrochemical assessment of groundwater using multivariate statistical methods and water quality indices (WQIs)'. **Applied Water Science**, [*s. l.*], v. 14, n. 33, 2024. DOI: https://doi.org/10.1007/s13201-023-02084-0.

ISAAKS, E. H.; SRIVASTAVA, R. M. **An Introduction to Applied Geostatistics**. New York: Oxford University Press, 1989.

KHELALFA, M.; BOUCHAHM, N.; CHAIB. W. Management of groundwater resources in the Tolga region (south-east Algeria). **Studies in Engineering and Exact Sciences**, [*s. l.*], v. 5, n. 2, p. e11650, 2024.DOI: http://doi.org/10.54021/seesv5n2-650.

LAOUFI, A. ; GUETTAIA, S. ; BOUDJEMA, A. ; DERDOUR. A.; ALMALKI, A. S.; BOJER, A. K.; EL-NAGDY, K. A.; ALI, E. Seasonal groundwater quality analysis in a drought prone agricultural region using GIS and IWQI for nitrate contamination insights. **Scientific Reports**, [*s. l.*], v. 15, n. 1, 22948, 2025. DOI: https://doi.org/10.1038/s41598-025-06884-z

MANSOURI, Z.; DINAR, H.; BELKENDIL, A.; BAKELLI, O.; DRIAS**,** T.; ASSADI, A. A.; KHEZAMI, L.;MOUNI, L. 'Integrated Groundwater Quality Assessment for Irrigation in the Ras El-Aioun District: Combining IWQI. GIS. and Machine Learning Approaches'. **Water**, [*s. l.*], v. 17, n. 11, 1698, 2025**.** DOI: https://doi.org/10.3390/w17111698

MEIRELES, A. C. M.; ANDRADE, E. M. D.; CHAVES, L. C. G.; FRISCHKORN, H.; CRISOSTOMO, L. A. 2010. A new proposal of the classification of irrigation water**. Revista Ciência Agronômica**. Fortaleza, v. 41, n. 3, p.349–357, 2010. DOI: https://doi.org/10.1590/S1806-66902010000300005.

MESSAID, N.; HADJAB, R;. KHAMMAR, H. ; HADJAB, A. ; BOUCHEMA, N. ; CHEBOUT, A. R.; AQNOUY, M.; TZORAKI, O.; BENAABIDATE, L. Assessment of groundwater quality for irrigation in the semi-arid region of Oum El Bouaghi (northeastern Algeria) using groundwater quality and pollution indices and GIS techniques. **Water**, [*s. l.*], v. 17, n. 22, 3266. 2025. DOI: https://doi.org/10.3390/w17223266

MISHRA, A.; MISHRA, P. K.; MISHRA, A.; PANDEY, H. K.; ABDELRAHMAN, K.; FNAIS, M. S. Spatio-temporal characterization of groundwater hydrogeochemistry using GIS. multivariate statistics and geochemical modeling in the Lower Ganga-Yamuna Doab region. India. **Applied Water Science**, [*s. l.*], v. 15, n. 10, 262, 2025. DOI: https://doi.org/10.1007/s13201-025-02448-8

MURHULA, M.; KUTANGILA, M.; BIRHENJIRA, M.; MUYISA. K. Hydrogeochemistry and susceptibility to groundwater contamination in the Panzi sector. Bukavu City. DR Congo. **Geo-Eco-Trop**, [*s. l.*], v. 43, n. 1, p. 197-209, 2019.

NEFLA, L.; BERGAL, A.; BOUMARAF, W.; GHEID, S.; BOUKSIBA, C.; KHAMMAR, H.; CELICO, F.; NASRI, H.; GAAGAI, A.; ELSAYED, S.; ABD EL-BAKI; M. S.; ATTIAH, A. M.; SZÉKÁCS, A.; SAEED, O.; GAD, M.Integrated GIS-machine learning approach to irrigation water quality assessment in coastal aquifers. **Scientific Reports**, [*s. l.*], v. 16, 3894, 2026. DOI : https://doi.org/10.1038/s41598-025-25461-y

OSS. **Système aquifère du Sahara septentrional (SASS)**: gestion concertée d'un bassin transfrontalier. Tunis: OSS, 2003.

REGHAIS, A.; DROUICHE, A.; ZAHI, F.; EWUZIE, U.; DEBIECHE,T.-H.; DRIAS, T. Risk assessment of potentially toxic elements and mapping of groundwater pollution indices using soft computer models in an agricultural area. Northeast Algeria. **Journal of Hazardous Materials**, [*s. l.*], v. 491, 137991, 2025. DOI: http://doi.org/10.1016/j.jhazmat.2025.137991.

TANG, L.; YAO, R.; ZHANG, Y.; DING, W.; WANG, J.; KANG, J.; LIU, G.; ZHANG, W.; LI, X. 'Hydrochemical analysis and groundwater suitability for drinking and irrigation in an arid agricultural area of Northwest China'. **Journal of Contaminant Hydrology**, [*s. l.*], v. 259. 104256, 2023. DOI: https://doi.org/10.1016/j.jconhyd.2023.104256.

TIAN, J.; YANG, J.; LIU, W.; ZHANG. M.; DASKALOPOULOU, K. ; ZOU, Y.; XU, N.; LIAO, Z.; HUO, Y.; ZHU, Y.; CAO, Y.; XU, S.; LI, J. 'Assessing groundwater quality for drinking and irrigation using hydrogeochemistry and machine learning in Northern China'. **Agricultural Water Management,** [*s. l.*], v.322, 109975, 2025. DOI : https://doi.org/10.1016/j.agwat.2025.109975.

UNESCO. **Étude des ressources en eau du Sahara septentrional.** Paris: UNESCO, 1972.

WEBSTER, R.; OLIVER. M. A. **Geostatistics for Environmental Scientists**. 2nd ed. Chichester: John Wiley & Sons, 2007.

YANG, X. ; LI, H. ; ZHANG, Y. *et al*. Hydrogeochemical characterization and quality assessment of groundwater based on integrated-weight water quality index in a concentrated urban area. **Environmental Systems Research,** [*s. l.*], v. 11, n. 1, p.1, 2022. DOI: http://doi.org/10.1186/s40068-022-00257-2.

ZOUAOUI, S.; MENANI, M. R.; GAAGAI, A.; BOUABID, A.; BENCEDIRA, S.; ZEKKER, I.; AOUISSI, H. A. Contribution of stable isotopes to the study of groundwater recharge in the southern foothills of the Saharan Atlas: the case of Tolga Region. North Eastern Algeria. **Research Square (preprint),** [*s. l.*], 2022. DOI: http://doi.org/10.21203/rs.3.rs-1869669/v1.